Hindawi
Advances in Civil Engineering
Volume 2020, Article ID 8813303, 12 pages
https://doi.org/10.1155/2020/8813303

Research Article

Numerical Study on the Longitudinal Response Characteristics of Utility Tunnel under Strong Earthquake: A Case Study

Guoyi Tang,[1] Yumei Fang,[1] Yi Zhong,[2] Jie Yuan,[3] Bin Ruan,[2] Yi Fang,[3] and Qi Wu[4]

[1]*The 1st Geological Brigade of Jiangsu Geology and Mineral Exploration Bureau, Nanjing 210009, China*
[2]*School of Civil Engineering and Mechanics, Huazhong University of Science and Technology, Wuhan 430074, China*
[3]*Institute of Crustal Dynamics, China Earthquake Administration, Beijing 100085, China*
[4]*Institute of Geotechnical Engineering, Nanjing Tech University, Nanjing 210009, China*

Correspondence should be addressed to Jie Yuan; yuenjay@sina.cn

Received 24 May 2020; Revised 23 July 2020; Accepted 31 July 2020; Published 20 August 2020

Academic Editor: Peixin Shi

Copyright © 2020 Guoyi Tang et al. This is an open access article distributed under the Creative Commons Attribution License, which permits unrestricted use, distribution, and reproduction in any medium, provided the original work is properly cited.

In this paper, the longitudinal seismic response characteristics of utility tunnel subjected to strong earthquake was investigated based on a practical utility tunnel project and numerical method. Firstly, the generalized response displacement method (GRDM) that was used to conduct this study was reviewed briefly. Secondly, the information of the referenced engineering and the finite element model was introduced in detail, where a novel method to model the joints between utility tunnel segments was presented. Thirdly, a series of seismic response of the utility tunnel were provided, including inner force and intersegment opening width. The results showed that (i) the seismic response of the utility tunnel under far-field earthquake may be remarkable and even higher than that under near-field earthquake; (ii) sharp variation of response may occur at the interface between "soft" soil and "hard" soil, and the variation under far-field earthquake could be much more significant. This research provides a reference for the scientific study and design of relevant engineering.

1. Introduction

The utilization of underground space can help cities solve those problems which arise from urbanization and population growth, for example, costly and limited surface space [1]. Since the last decade, utility tunnels are being used to settle the problems of many cities, such as Paris, Tokyo, Madrid, and Hamburg. The utility tunnel has become one of the most important lifeline engineering in modern cities, in which a lot of lifeline systems are contained, including heating pipe, water supply, power cable, gas pipeline, and telecom. In 1985, a utility tunnel of 1706 m was built in Beijing; since then, a large number of utility tunnel projects have been constructed or planned in China. It was announced at the Fourth Session of the Congress of the People's Republic of China in the Report on the Work of the Government that construction will begin on at least 2000 km of utility tunnels during 2016 [2].

Besides, in China, utility tunnels are usually constructed in large cities that are located in seismically active areas. Then, the underlying earthquake hazards would stand a severe threat to the safety and operation of the utility tunnels. In the 1995 Hyogoken-Nambu earthquake, various types of damage were observed on the utility tunnel, such as cracks, joints dislocation, and concrete layer spalling [3, 4]. Hashash et al. [5] indicated that underground structures might also be subjected to severe damage under earthquake and emphasized the importance of aseismic design of underground structures. Therefore, a lot of researchers have conducted studies on the seismic behavior of underground tunnels.

Park et al. [6] developed a longitudinal displacement profile-based procedure for simulating the tunnel response under spatially varying ground motion. Amorosi and Boldini [7] carried out simulation of a group of shallow tunnels and the mechanical characteristic under the dynamic action was reproduced, using a new constitutive model of soil and tunnel lining. Hleibieh et al. [8] simulated the centrifugal experiment of a tunnel buried in sand and studied the

seismic response of tunnel and sand under the action of earthquake. Tsinidis et al. [9] used the nonlinear soil-tunnel interface model to investigate the influence of tunnel lining stiffness on the dynamic response of the soil-tunnel system. Patil et al. [10] used the finite element method to study the seismic response of the tunnel under the condition of soft soil foundation and compared it with the available analytical solution. Chen et al. [11, 12] investigated the seismic performance of utility tunnel under nonuniform earthquake wave excitation through a series of model tests and numerical simulations; the shear force-slip relationship at the soil-model structure interaction surface, movement and rotation of the construction joint, and the effect of nonuniform earthquake input were discussed. Considering the passage of Rayleigh wave, Li et al. [13] studied the dynamic response of the utility tunnel through the finite-element method and demonstrated that the utility tunnel exhibited global bending deformation under Rayleigh wave, and Rayleigh wave can be an essential factor in controlling the damage of the tunnel. Jiang [14] presented a view of the current state of studies on the seismic response of utility tunnels and outlined the future scope of work on the subject.

In addition, the longitudinal response characteristics of extended underground tunnels have also attracted wide attention. Different from the transverse direction, there are more factors to be considered in the longitudinal direction, including parameters and distribution of soil and size of model. And the yield and failure of connectors between segments may lead to unexpected deformation or damage of the large-scale tunnel along the longitudinal direction, so it is necessary to study the longitudinal response characteristics. Li and Song [15] studied the numerical modeling techniques for the analysis of the longitudinal response of tunnels under an asynchronous seismic wave. Chen et al. [16] reported a study on the nonlinear response characteristics of undersea shield tunnel subjected to strong earthquake motions. Miao et al. [17–19] studied the spatial distribution characteristics of longitudinal response of the shield tunnel under multiple support excitations. In summary, studies on the longitudinal response characteristics of large-scale utility tunnels are still rare and are also of great significance. Tsinidis et al. [9] used a nonlinear soil-tunnel interface model to conduct dynamic centrifugal numerical tests on a flexible circular tunnel model buried in dry sand to study the influence of tunnel lining stiffness on the dynamic response of the soil-tunnel system. Zhang et al. [20] carried out tunnel shaking table tests on the combined position of the shaft and tunnel, using different synthetic ground motions as seismic excitations to study the acceleration response of shafts and tunnels. Chen et al. [21] carried out a series of shaking table tests to study the seismic performance of transition tunnel structures and discussed the influence of changes in section and stiffness on the seismic response of the tunnel area.

For this complex problem of the seismic longitudinal response of large-scale utility tunnels, it is difficult to establish a three-dimensional refined finite element model for overall time history analysis because of the complexity of the modeling process, the low efficiency of calculation, the difficulty of postprocessing, and the slow speed of data extraction. In engineering practice, the simplified method for seismic response of tunnel is usually used. Although the commonly used method is simple in calculation and few in parameters, a lot of simplification in soil and structure is often done, reducing the calculation accuracy. In order to analyze the seismic longitudinal response characteristics of large-scale utility tunnel in complex engineering site quickly and accurately, efforts have been made in calculation and modeling methods here, providing reference for the modeling method and seismic design of utility tunnels. And compared with the previous work, more factors will be considered here, such as the nonlinearity of soil, the nonuniformity of soil distribution, and the influence of prestressed steel strand.

Taking a practical engineering as reference, a numerical investigation on the longitudinal seismic response characteristics of the utility tunnel was conducted. The method that we used to carry out the numerical study was reviewed first. Then, the relevant information of the large-scale soil-utility tunnel finite-element model we established was given in detail, including model dimension, material properties, boundary conditions, and wave selection. Moreover, a series of seismic responses of the utility tunnel were presented and analyzed, where the spatial distribution characteristics of longitudinal response of utility tunnel was focused on. At last, concluding remarks were outlined.

2. Review of Methodology

The authors extended the concept of response displacement method (RDM) specified in "Code for seismic design of urban rail transit structures" (Chinese National Standard, GB50909-2014) and proposed the generalized response displacement method (GRDM) [22]. The response displacement method assumes that the displacement of the ground in the longitudinal direction of the tunnel during the earthquake is sine distribution and simulates the tunnel with beam elements or rod elements. The action of the ground spring is applied to the tunnel in the form of static force to calculate the internal force, stress, and displacement of the tunnel. The stratum displacement distributed according to the sine function is expressed by amplitude and wavelength. The amplitude can be solved by the response spectrum method or time history analysis method. When the stratum conditions around the tunnel vary greatly along the longitudinal direction of the tunnel, it is not appropriate to assume that the displacement along the longitudinal direction of the tunnel is sine distribution. Instead, the time history analysis method should be used to calculate the actual displacement distribution of the stratum along the longitudinal direction of the tunnel and then force it to the load form of displacement acts on the analysis model, which is the (GRDM). Basically, the GRDM contains two steps for calculating the response of underground structures. First, a 2D (two-dimensional) free-field model is established, where the position and existence of underground structures was considered in meshing work, and then the free-field response was calculated and extracted. Second, a soil-underground structure model represented by springs and beam

elements was constructed; the extracted free-field response was then inputted into this model, and the seismic response of the underground structure can be obtained. As a matter of fact, the GRDM is a refined RDM and gives the RDM the ability to conduct large-scale simulation. The GRDM is based on the actual displacement of the stratum along the longitudinal direction of the tunnel. Compared with the RDM, more factors can be considered through the GRDM. The GRDM method can consider the inhomogeneity of the soil layer and multipoint ground motion input. And compared with 3D Dynamic transient analysis, the effectiveness of GRDM is verified in Chen et al. [16]. Detail information about the GRDM can be found in [17, 18]. Overall, this method has wide applicability and can be used to analyze the seismic dynamic response of various large-scale underground structures, including the utility tunnel.

3. Numerical Model

3.1. Engineering Background and Wave Selection. The utility tunnel project of Jiangbei New area in Nanjing city, China was selected as the reference engineering. The soil layer distribution of the engineering site and the path of the utility tunnel are shown in Figure 1. As can be seen, the tunnel crosses different types of soils, which would be a key issue in the simulation. The tunnel was constructed with numerous rectangular concrete segments which were connected using prestressed steel strands (see Figure 2).

Nanjing city is located in the east coast of China where earthquake activity is high. Huaiyin-Xiangshui fault zone, Tancheng-Lujiang fault zone, and Luan fault zone are located to the north, northwest, and west of Nanjing city, respectively. The epicenters of historical destructive earthquake events occurred in this area are presented in Figure 3. It is can be found that Nanjing city was mainly subjected to far-field earthquakes, and the near-field earthquakes were relatively fewer. Therefore, the seismic response under far-field earthquakes should be emphasized. This area experienced 306 earthquakes (moment magnitude ≥2) from January 1970 to December 2013, and the number of those earthquakes with focal depth of 20–30 km is up to 214 (about 70% of the total number). Thus, that focal depth ranging from 20 to 30 km was set as a wave selection condition in the numerical simulation. Besides, an underground utility tunnel was focused on in this paper, so borehole records should be used; taking the site conditions (especially the depth of base rock) into account, that borehole depth ≥100 m was set as another wave selection condition. According to "Code for seismic design of buildings, GB 50011-2010" (Chinese National Standard, GB 50011-2010) [23], the design basic acceleration of ground motion for Nanjing city is set as 0.1 g (1 g = 9.8 m/s^2). Therefore, extra selection criteria were set and presented as follows: moment magnitude ≥6 and the PGA (Peak Ground Acceleration) of horizontal component ranging from 0.1 g to 0.2 g. The borehole records from Kiban-Kyoshin network (KiK-net) in Japan were used for input motion selection.

3.2. Numerical Model of Free-Field

3.2.1. Setup of the Numerical Model. A 2D free-field model was established completely according to the practical site conditions (see Figure 1) to describe thoroughly the soil layers distribution. The dimension of the free-field model is 1500 m × 80 m. 4-node quadrilateral elements (CPE4R) and 3-node triangular elements (CPE3) were employed to discretize the model. Herein, the triangular elements were adopted to implement mesh transition in some extremely complex parts of the model. The numbers of quadrilateral elements and triangular elements are 219252 and 245, respectively. Abaqus/Explicit platform was used to proceed with the calculation.

3.2.2. Boundary Conditions and Input Earthquake Motions. Viscous-spring artificial boundary was adopted on the bottom and lateral boundaries of the 2D model to eliminate the boundary effect [24]. The NS and vertical components of Shizuoka and Tochigi waves were selected as input excitation according to the abovementioned selection criteria, which represented the near-field and far-field earthquakes, respectively. The information of these two records is shown in Table 1. Note that the equivalent node force derived from selected ground motions was finally inputted into the model. The waveform, significant duration, Fourier spectra, and response spectra of selected earthquake records were plotted in Figure 4. The peak value of input ground motion was adjusted to 0.05, 0.1, 0.2, and 0.4 g to observe the tunnel response versus increasing PGA.

3.2.3. Constitutive Model. To simulate the nonlinearity of the soil, the three-parameter modified Davidenkov model is used here. This constitutive model follows the "upper skeleton curve" rule in the "Extended Masing" rule. And the loading and unloading criteria of the hysteresis curve is modified based on the "n times method" proposed by Pyke et al. [25]. In addition, the calculation efficiency is enhanced without losing the calculation accuracy through improving the equivalent strain algorithm of the modified Davidenkov model. And the modified Davidenkov model was made use of to describe the nonlinear dynamic properties of soils in this site [26–29]. Combining the Davidenkov model with a large number of resonant column tests, the parameters involved in this constitutive model were obtained and given in Table 2. The stress-strain hysteretic curve for the modified Davidenkov model is shown in Figure 5(a), while the curves of dynamic shear modulus ratio versus shear strain ($G/G_{\max}$-γ) and damping ratio versus shear strain (λ-γ) are plotted in Figure 5(b).

3.3. Numerical Model of Soil-Tunnels System. As stated in Section 2, a 3D soil-utility tunnel system represented by springs and beam elements was established after the simulation of seismic response of the 2D free-field model. The soil-tunnel model was also 1500 m long. As shown in Figure 6, the 3D soil-utility tunnel model was constructed using

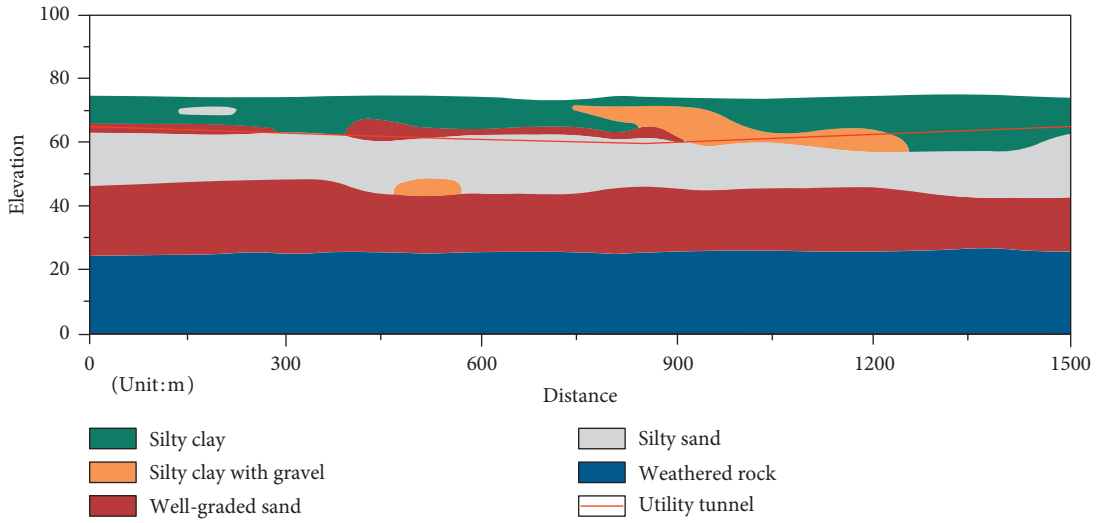

Figure 1: Soil layers of the engineering site.

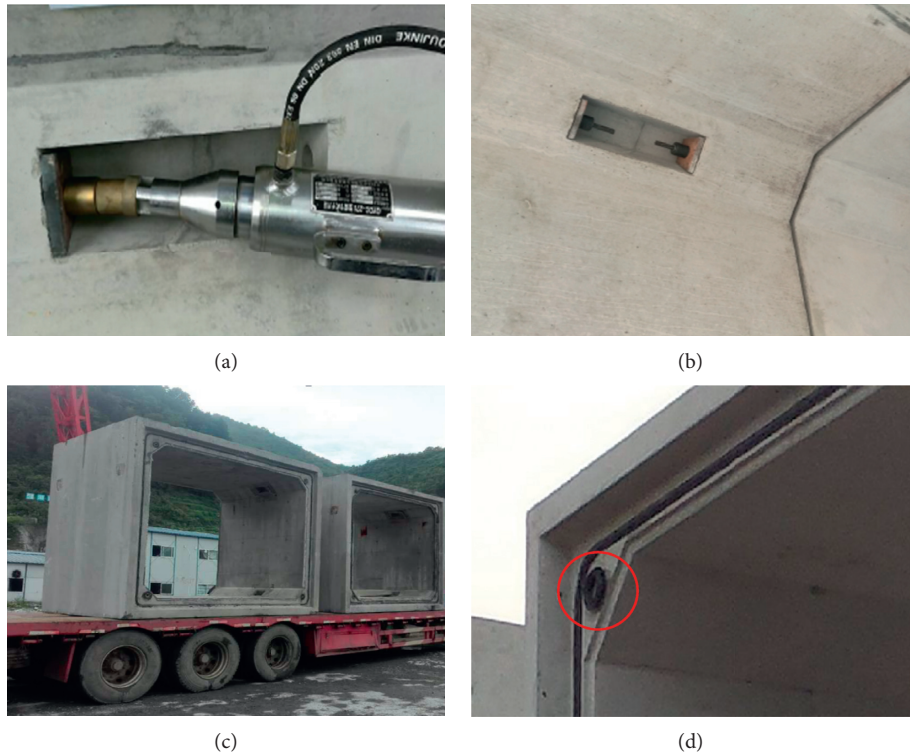

Figure 2: Photos of the utility tunnel segment and prestressed steel. (a) Prestress installation process. (b) Prestressed steel position. (c) Prefabricated utility tunnel. (d) Prestressed steel hole.

numerous concrete segments, prestressed steels, and soil springs. Each segment was 1.5 m long in the longitudinal direction, and the number of segments was 1000. Concrete properties are shown in Table 3 and these parameters related to the soil-utility tunnel system all come from the actual project. The segment was discretized using elastic 3D hollow Timoshenko beam element that allows for transverse shear deformation, and each segment contained two beam elements (each beam element was 0.75 m in length). The dimensions of the segment cross-section can be found in Figure 6. Soil springs were employed to model dynamic soil-tunnel interaction. For each segment, four tridirectional soil springs were set at the top, bottom, and two lateral boundaries, respectively. The number of the soil springs was 4000. Note that one end of the soil spring was fixed, while the other end was located at the middle node of the two beam elements. The calculation method of the stiffness of soil springs for different soil types was provided [16–18]:

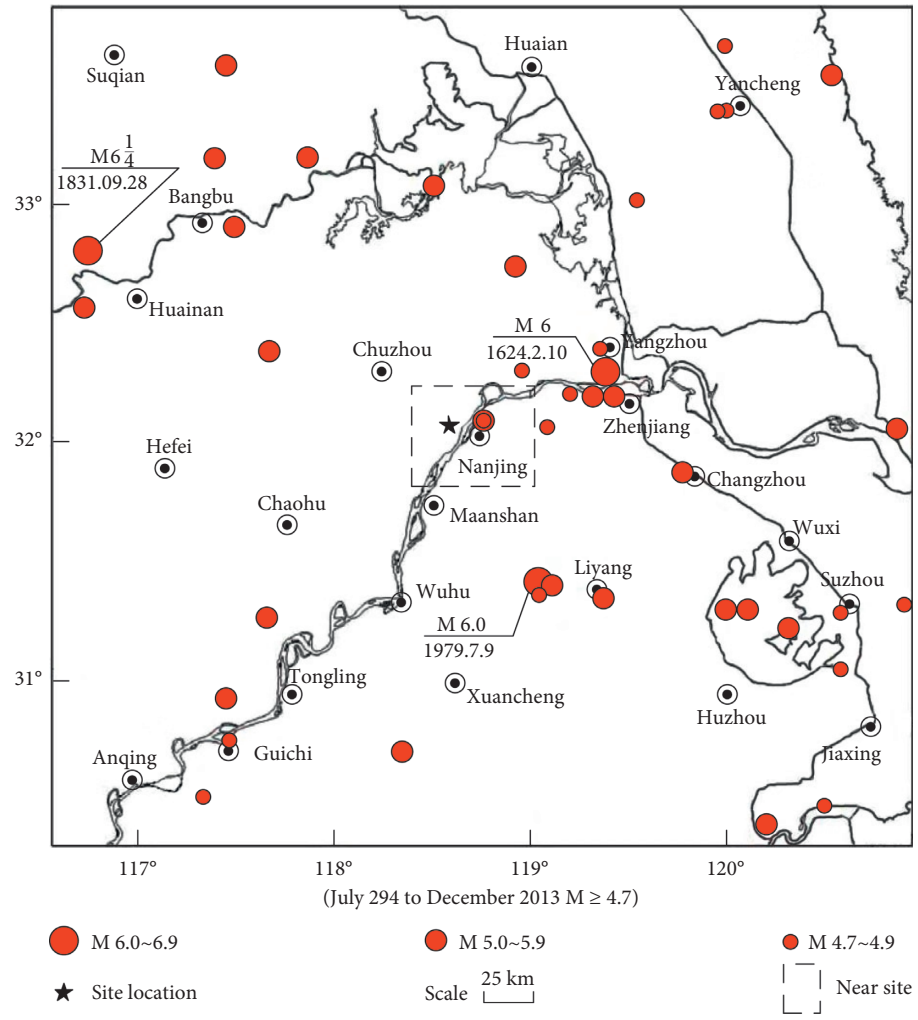

Figure 3: Historical earthquake events in this area.

Table 1: Information of the selected ground motions.

Ground motion information	Shizuoka wave	Tochigi wave
Event time (yy/mm/dd/ hh:mm)	2009/08/11/ 05:07	2011/03/11/ 14:46
Moment magnitude	6.5	9.0
Focal depth (km)	23	24
Focal distance (km)	24.705	300.51
Station code	SZOH39	TCGH16
Borehole depth (m)	103	112
Bedrock shear wave velocity (m/s)	1500	680
Selected horizontal component	NS	NS
Horizontal PGA (g)	0.124	0.181
Vertical PGA (g)	0.057	0.140

$$K_t = 3G_u,$$
$$K_1 = \beta K_t, \quad (1)$$

where K_t and K_l are spring coefficients per unit length perpendicular to and parallel to the soil layer, respectively; G_u denotes the shear modulus of foundation soil corresponding to the maximum strain amplitude of earthquake vibration; and β is a constant which can be set to 1/3.

Herein, a novel joint modeling method was adopted. In the referenced engineering, four prestressed steel strands are used to constrain the adjacent two tunnel segments (see Figure 2), and the strengthening stress for each strand is 120 MPa. In this paper, one Timoshenko beam element was utilized to model the prestressed steel strands between any two adjacent segments (see Figure 6). Therefore, the strengthening stress of 480 MPa was applied to the beam element for prestressed steel. Opposite to the engineering practice, compression was performed on each beam element for prestressed steel strand to model the constraint effect. The number of the beam elements for modeling prestressed steel was 999. The properties for these beam elements are presented in Table 4. This joint modeling method can reflect the real connection conditions, and the simulation results shown in Section 4 demonstrate its application effect.

The extracted horizontal and vertical displacement responses from the 2D free-field model were inputted into the soil-tunnel model to calculate the tunnel response. Note that

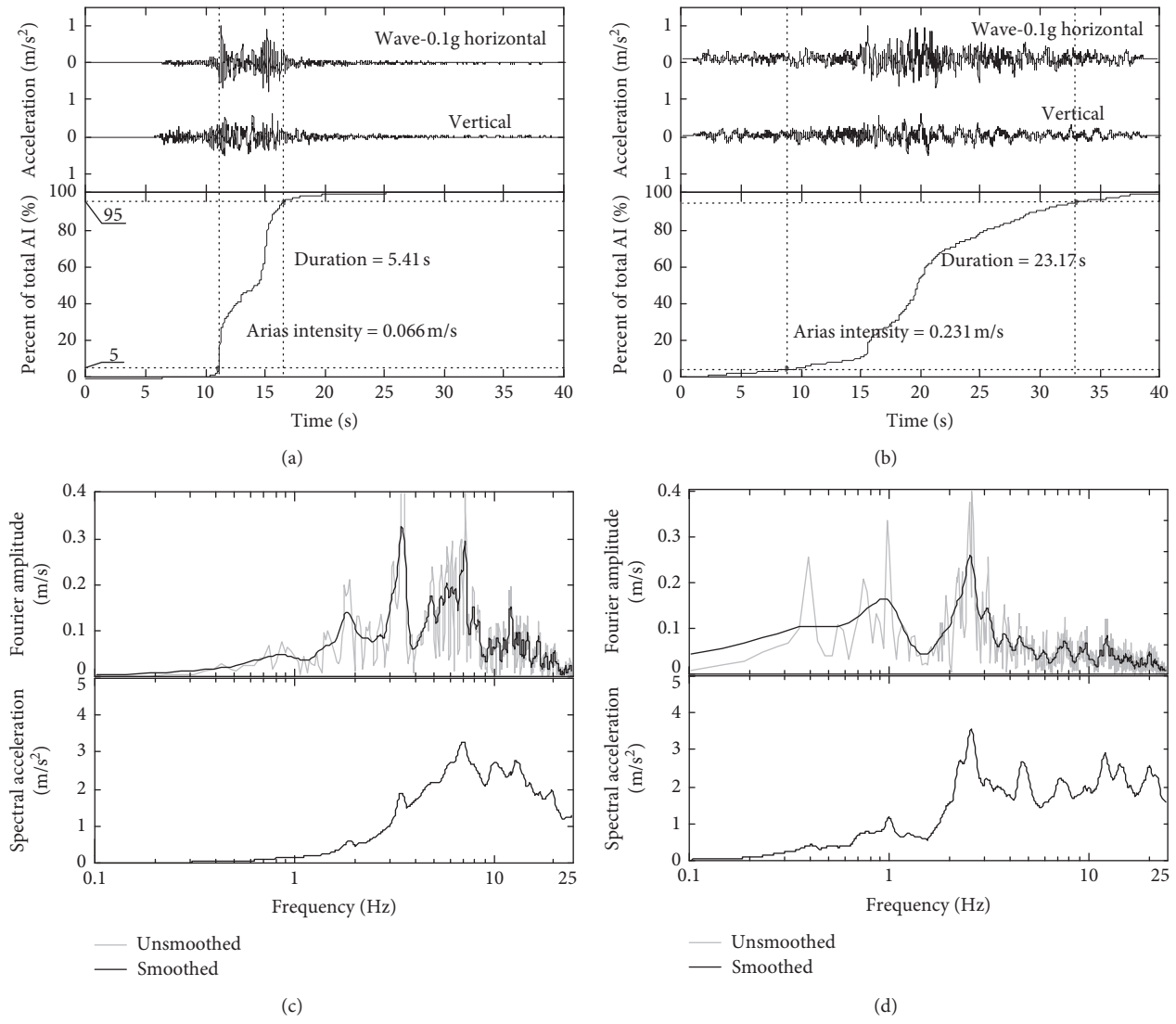

Figure 4: The waveform, significant duration, Fourier spectra, and response spectra of selected earthquake records: (a) time history and significant duration of Shizuoka wave; (b) time history and significant duration of Tochigi wave; (c) Fourier and response spectra of Shizuoka wave; (d) Fourier and response spectra of Tochigi wave.

Table 2: Soil properties.

Soil types	Fitting parameters			Density (kg/m^3)	G_{max} (Pa)	Poisson's ratio
	A	B	γ_0 ($\times 10^{-4}$)			
Silty clay	1.09	0.41	3.72	1920	39262080	0.32
Silty clay with gravel	1.05	0.42	3.43	1960	68539240	0.31
Well-graded sand	1.04	0.40	6.44	1980	174653820	0.28
Silty sand	1.01	0.35	7.67	1990	249529500	0.24
Weathered rock	1.01	0.38	10.04	2000	1280000000	0.38

the extracted horizontal displacement response was inputted simultaneously in both the transverse and longitudinal directions to obtain more conservative results [30].

4. Results and Discussion

The compression stress, tensile stress, bending moment, shear stress, and intersegment opening width response of the utility tunnel were calculated and presented in Figures 7–11, respectively, where the intersegment opening width at certain location was defined as the maximum relative distance between adjacent two segments in the whole duration. In general, the responses under far-field earthquakes are higher than those under near-field ones, which seems to be opposite to some previous research studies, for instance, Chen and Wei [31] and Chen et al. [32]. This is because that

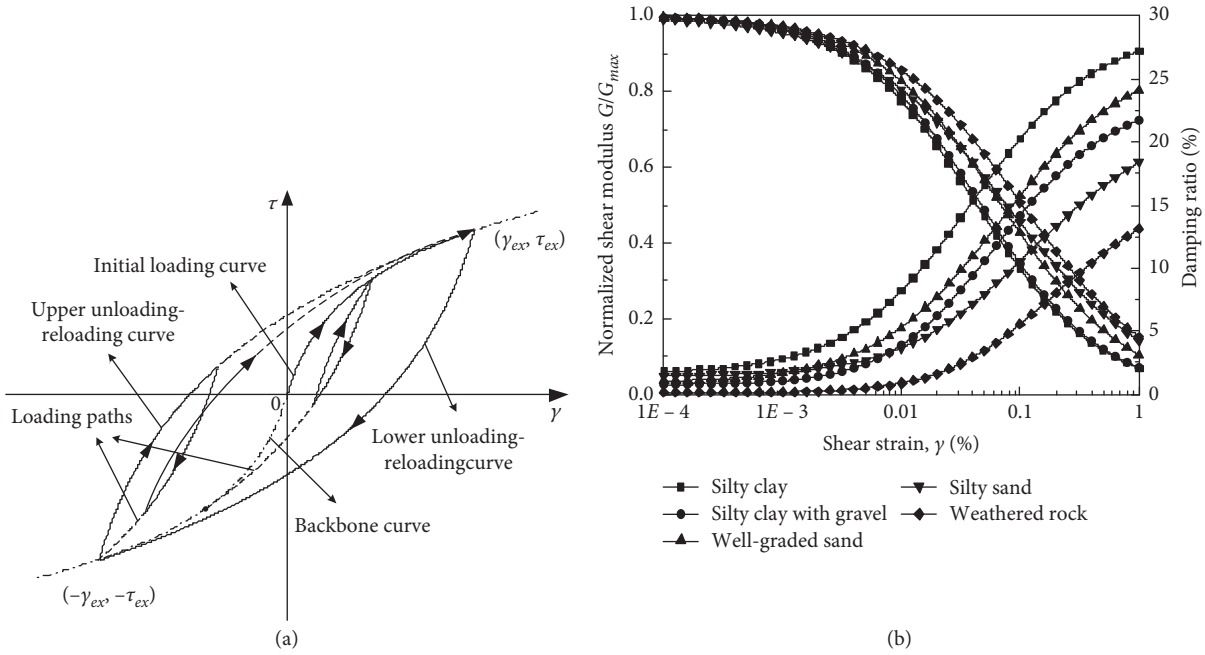

Figure 5: The modified Davidenkov model: (a) stress-strain hysteretic curve; (b) $(G)/(G)_{max}$-γ and λ-γ curves of soils.

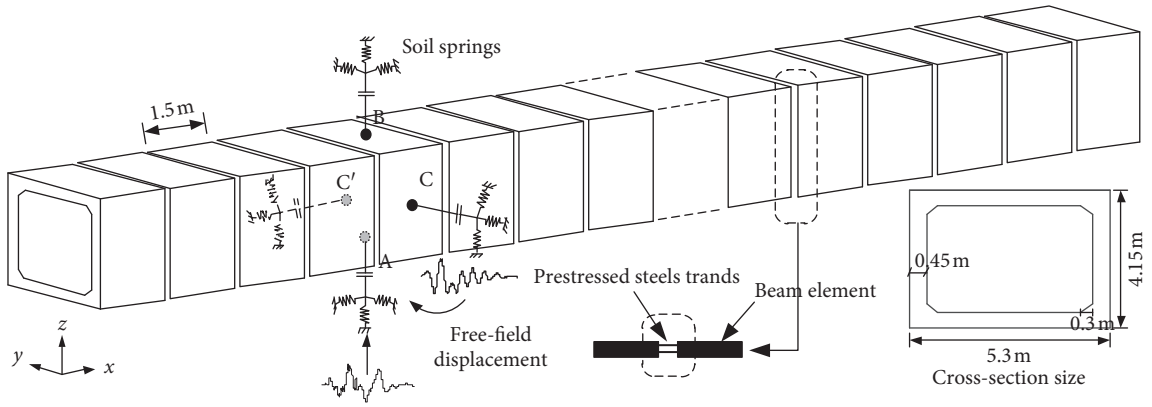

Figure 6: Schematic diagram of the utility tunnel model.

Table 3: Concrete properties.

	Elastic modulus E_p (GPa)	Compressive strength f_c (MPa)	Tensile strength f_t (MPa)
C60	35.5	27.5	2.04

Table 4: Prestressed steel strand parameters.

	Tensile strength f_{ptk} (MPa)	Elastic modulus E_p (GPa)	Steel cross-sectional area mm^2
Φ^s15.2 (1 × 7)	1860	200	139 × 7

the moment magnitude and Arias intensity of the far-field wave are greatly higher than those of the near-field one. From the Fourier spectra and acceleration response spectral in Figure 4, the selected far-field waves contain more energy in the low-frequency band to which the utility tunnel is more sensitive. Besides, the significant duration of the far-field wave is much longer than that of the near-field one, which may also be an important factor. The spatial distribution of seismic response of the utility tunnel under far-field earthquake is greatly different from that, under near-field one due to the different spectral contents.

Moreover, as the input PGA increases, all the responses calculated increase. However, the increasing trend tends to be nonlinear due to the nonlinearity of the boundary conditions and soil constitutive model. The response distribution characteristics also significantly change with the increasing input PGA. The tunnel crosses different types of soil that possess different degrading tendencies; as the input

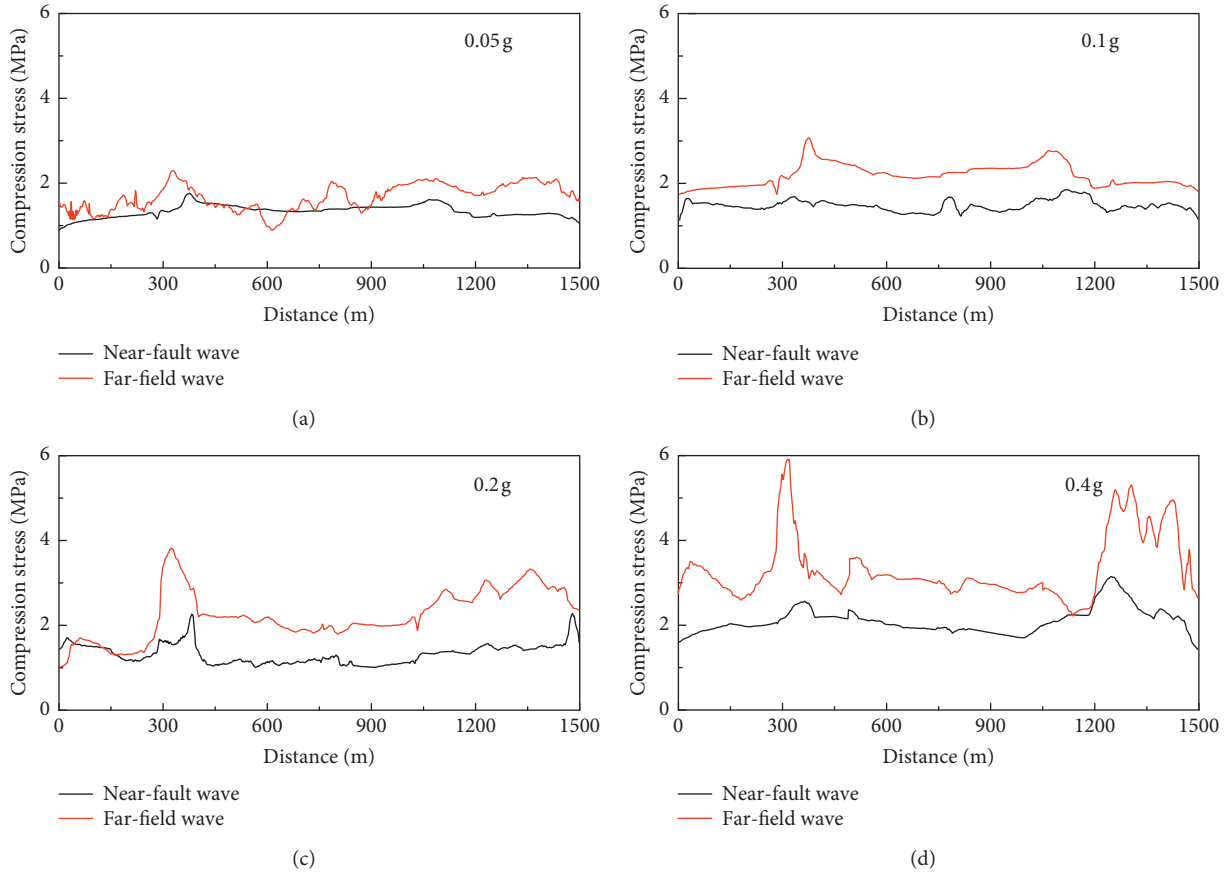

Figure 7: Compression stress response.

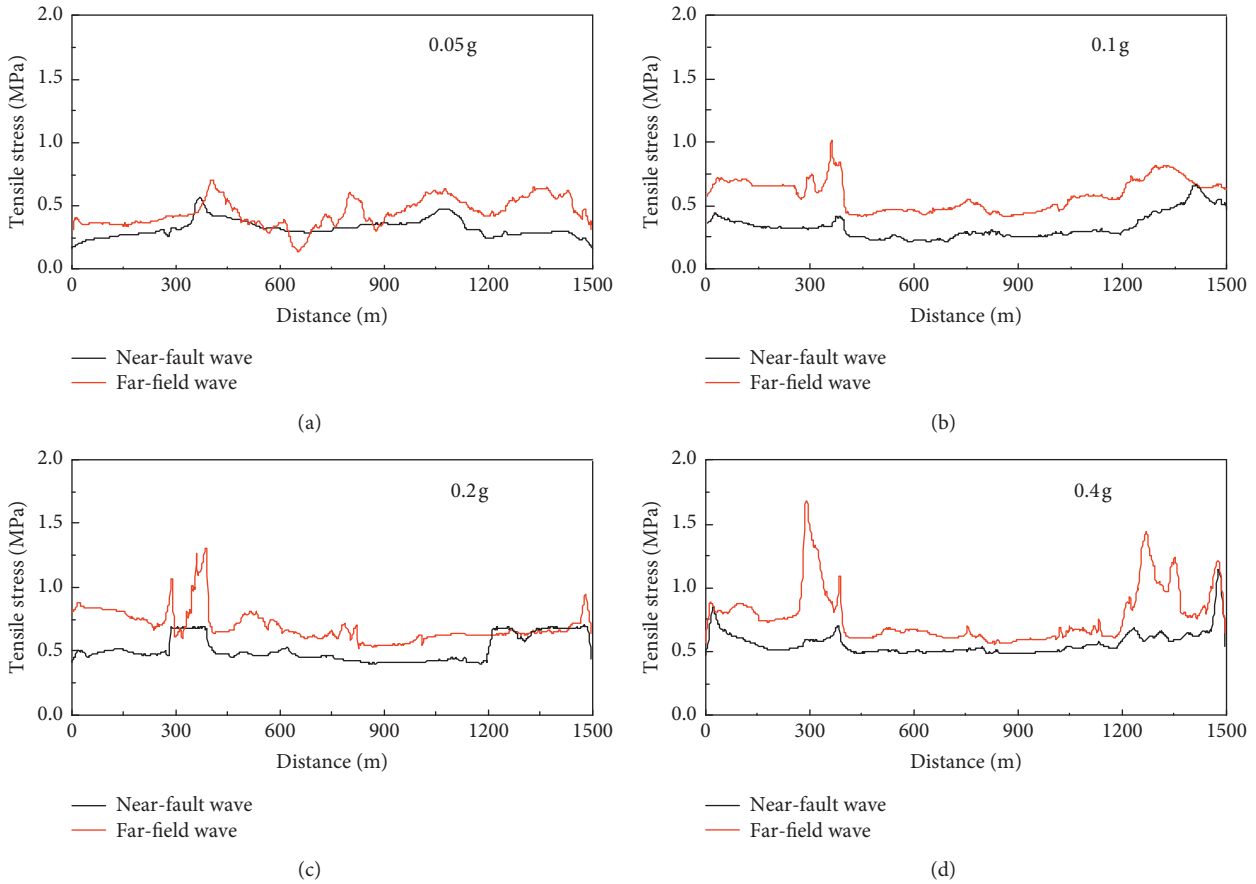

Figure 8: Tensile stress response.

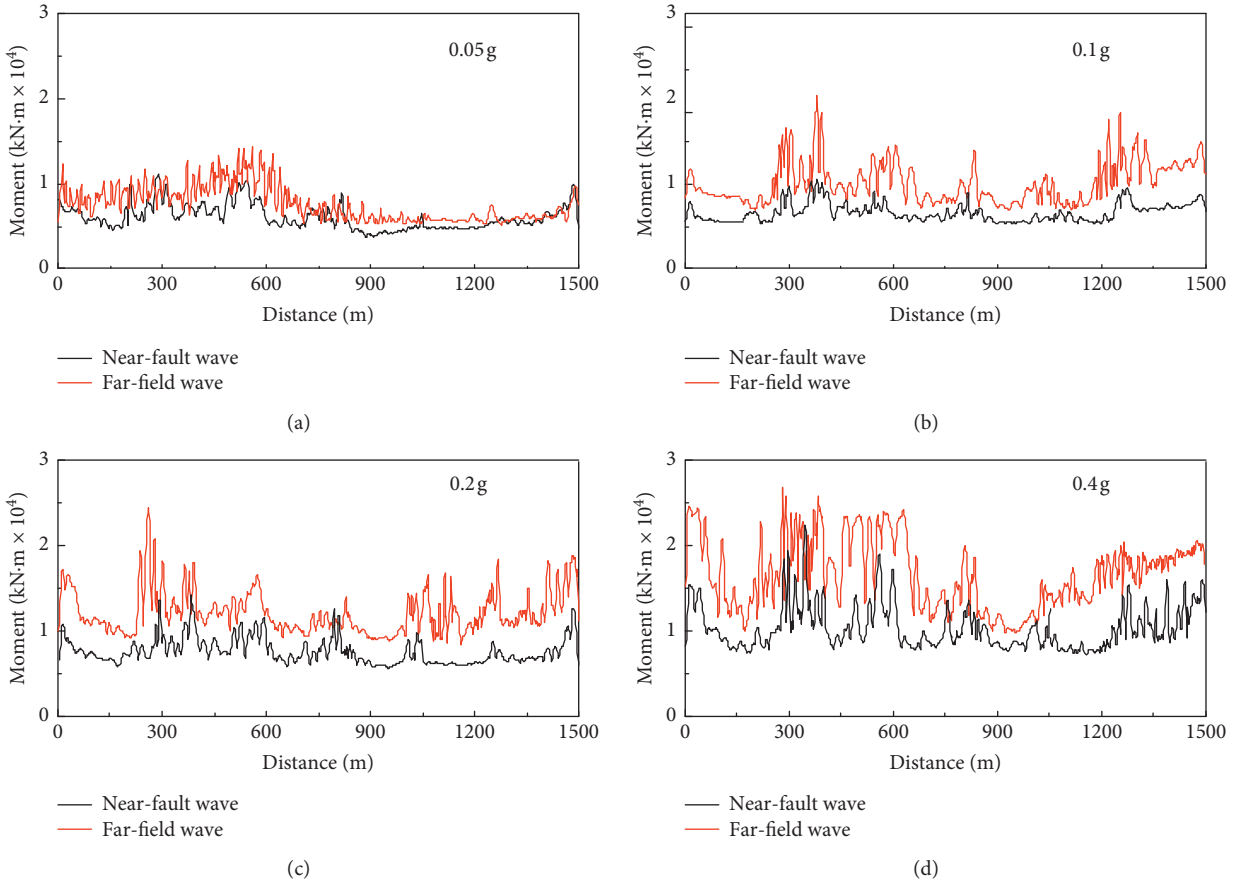

Figure 9: Bending moment response.

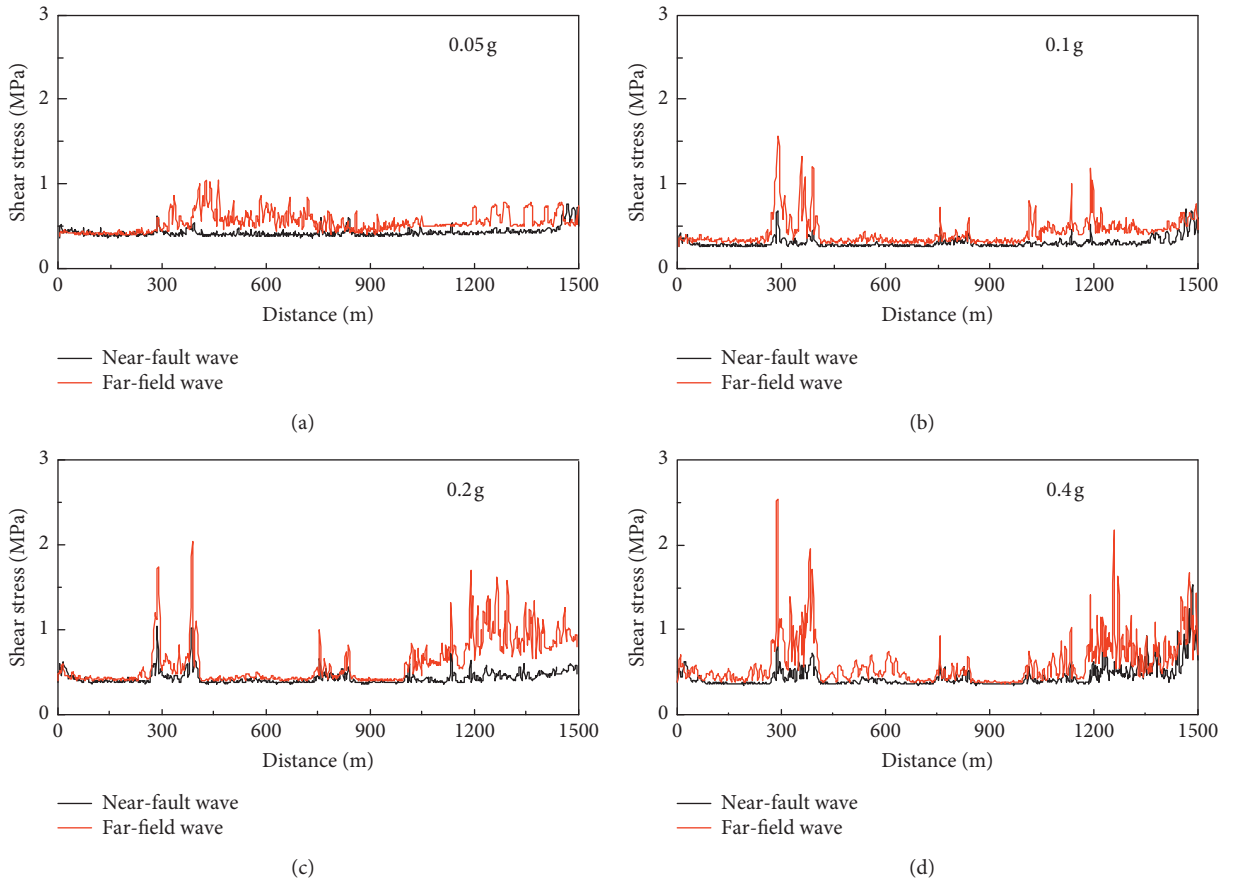

Figure 10: Shear stress response.

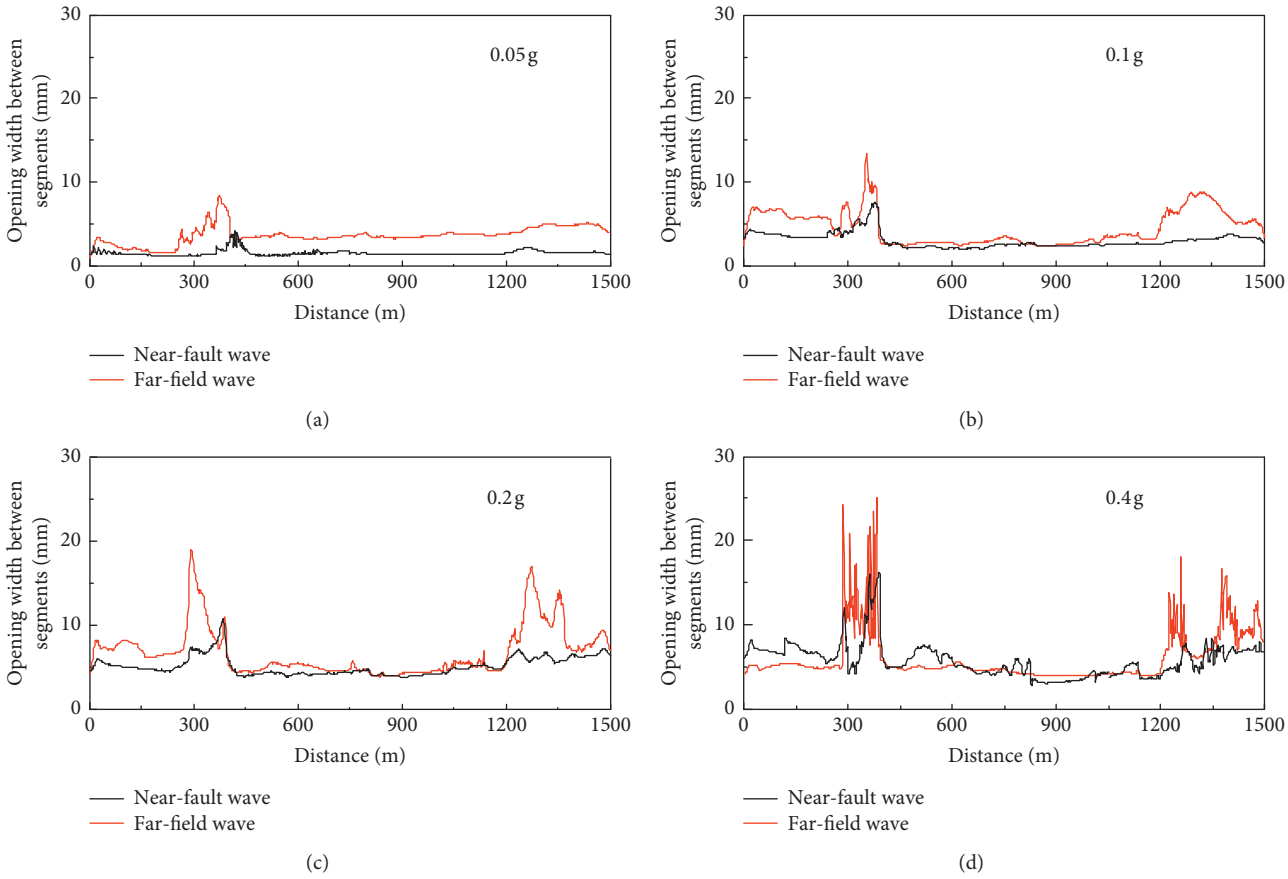

Figure 11: Intersegment opening width response.

PGA increases, some soil is damaged first so that it cannot resist the external load any longer, while some soil with higher stiffness may be still in the elastic state or damaged slightly so that it still can transit load as a medium.

In almost all the response curves, sharp variation shows up at about $D = 300$ m, 400 m, and 1200 m (D denotes distance) and this tendency tends to be more obvious as the input PGA increases and/or under the far-field earthquake. This can be attributed to the nonuniform distribution of soil layers on the path of the tunnel and different stiffness degrading tendencies of soil. Local soil property exhibits sharp variation: (i) the utility tunnel crosses silty clay layer and well-graded sand layer at about $D = 300$ and $D = 400$; (ii) the utility tunnel crosses silty clay layer and silty clay with gravel layer at about $D = 1200$. This results in the remarkably different site response and thus different tunnel response. Besides, it is believed that the spectral content can be another important influence factor because the response variation at the interface between two different types of soil under far-field earthquake is much larger than that under near-field one even though the input PGAs are the same. Therefore, for those utility tunnel projects in a complex site, both the seismic responses under near- and far-field earthquakes should be considered.

5. Conclusions

A series of numerical investigations were carried out on the seismic performance of the utility tunnel which is significantly critical for its safety and operation. The fundamental method (i.e., generalized response displacement method) was reviewed, and the information of the referenced utility tunnel project was introduced. The setup of the 2D and 3D models established was described in detail. The inner force response and intersegment opening width response of the utility tunnel were calculated. The main conclusions can be outlined as follows:

(1) A novel and simple modeling method of joint of the utility tunnel was proposed, and the simulation results demonstrated its application effect.

(2) Even though the input PGAs are the same, the seismic response of the utility tunnel under far-field earthquake is not necessarily lower than that under near-field one; the moment magnitude, Arias intensity, spectral content, and significant duration may have important influence on the intensity and spatial distribution characteristics of longitudinal response;

(3) Sharp variation of response of utility tunnel was observed at the interface between two different types of soil and corresponding seismic measures should be taken at these locations. The variation under the far-field earthquake was remarkably greater than that under the near-field one. Thus, far-field earthquakes could lead to more severe damage to the tunnel, and

the effect of far-field earthquake on the seismic response of utility tunnel crossing nonuniform site layers should be given more attention.

Data Availability

The raw data required to reproduce these findings cannot be shared at this time as the data also form part of an ongoing study.

Conflicts of Interest

The authors declare that they have no conflicts of interest regarding the publication of this paper.

Acknowledgments

This research was funded by Institute of Crustal Dynamics China Earthquake Administration (nos. ZDJ2020-08 and ZDJ2018-11) and National Natural Science Foundation of China (no. 41941016). The authors would like to thank Shanghai Railway Company of China Railway 17th Bureau for providing engineering materials.

References

[1] W. Broere, "Urban underground space: solving the problems of today's cities," *Tunnelling and Underground Space Technology*, vol. 55, pp. 245–248, 2016.

[2] T. Wang, L. Tan, S. Xie, and B. Ma, "Development and applications of common utility tunnels in China," *Tunnelling and Underground Space Technology*, vol. 76, pp. 92–106, 2018.

[3] S. Takada, N. Hassani, and M. Abdel-Aziz, "Quick report of main damage caused by the 1995 Hyogoken-Nambu earthquake," *Journal of Natural Disaster Science*, vol. 16, no. 3, pp. 59–70, 1995.

[4] A. J. Schiff, *Hyogoken-Nanbu (Kobe) Earthquake of January 17, 1995 Lifeline Performance. Technical Council on Lifeline Earthquake Engineering Monograph*, ASCE, Reston, VA, USA, 1998.

[5] Y. M. A. Hashash, J. J. Hook, B. Schmidt, and J. I-Chiang Yao, "Seismic design and analysis of underground structures," *Tunnelling and Underground Space Technology*, vol. 16, no. 4, pp. 247–293, 2001.

[6] D. Park, M. Sagong, D.-Y. Kwak, and C.-G. Jeong, "Simulation of tunnel response under spatially varying ground motion," *Soil Dynamics and Earthquake Engineering*, vol. 29, no. 11-12, pp. 1417–1424, 2009.

[7] A. Amorosi and D. Boldini, "Numerical modelling of the transverse dynamic behaviour of circular tunnels in clayey soils," *Soil Dynamics and Earthquake Engineering*, vol. 29, no. 6, pp. 1059–1072, 2009.

[8] J. Hleibieh, D. Wegener, and I. Herle, "Numerical simulation of a tunnel surrounded by sand under earthquake using a hypoplastic model," *Acta Geotechnica*, vol. 9, no. 4, pp. 631–640, 2014.

[9] G. Tsinidis, K. Pitilakis, and C. Anagnostopoulos, "Circular tunnels in sand: dynamic response and efficiency of seismic analysis methods at extreme lining flexibilities," *Bulletin of Earthquake Engineering*, vol. 14, no. 10, pp. 2903–2929, 2016.

[10] M. Patil, D. Choudhury, P. G. Ranjith, and J. Zhao, "Behavior of shallow tunnel in soft soil under seismic conditions," *Tunnelling and Underground Space Technology*, vol. 82, pp. 30–38, 2018.

[11] J. Chen, X. Shi, and J. Li, "Shaking table test of utility tunnel under non-uniform earthquake wave excitation," *Soil Dynamics and Earthquake Engineering*, vol. 30, no. 11, pp. 1400–1416, 2010.

[12] J. Chen, L. Jiang, J. Li, and X. Shi, "Numerical simulation of shaking table test on utility tunnel under non-uniform earthquake excitation," *Tunnelling and Underground Space Technology*, vol. 30, pp. 205–216, 2012.

[13] J. Li, Q. Yue, and J. Chen, "Dynamic response of utility tunnel during the passage of Rayleigh waves," *Earthquake Science*, vol. 23, no. 1, pp. 13–24, 2010.

[14] L. Z. Jiang, "State-of-the-Art of seismic response of utility tunnel," *Applied Mechanics and Materials*, vol. 353-356, pp. 2202–2205, 2013.

[15] P. Li and E.-X. Song, "Three-dimensional numerical analysis for the longitudinal seismic response of tunnels under an asynchronous wave input," *Computers and Geotechnics*, vol. 63, pp. 229–243, 2015.

[16] G. Chen, B. Ruan, K. Zhao et al., "Nonlinear response characteristics of undersea shield tunnel subjected to strong earthquake motions," *Journal of Earthquake Engineering*, vol. 24, no. 3, pp. 351–380, 2020.

[17] Y. Miao, E. Yao, B. Ruan, and H. Zhuang, "Seismic response of shield tunnel subjected to spatially varying earthquake ground motions," *Tunnelling and Underground Space Technology*, vol. 77, pp. 216–226, 2018.

[18] Y. Miao, E. Yao, B. Ruan, H. Zhuang, G. Chen, and X. Long, "Improved hilbert spectral representation method and its application to seismic analysis of shield tunnel subjected to spatially correlated ground motions," *Soil Dynamics and Earthquake Engineering*, vol. 111, pp. 119–130, 2018.

[19] Y. Miao, C. Chen, and B. Ruan, "Crossing-river shield tunnel longitudinal seismic response analysis based on generalized displacement method," *Journal of Beijing University of Technology*, vol. 44, no. 3, pp. 344–350, 2018, in Chinese.

[20] J. Zhang, Y. Yuan, and H. Yu, "Shaking table tests on discrepant responses of shaft-tunnel junction in soft soil under transverse excitations," *Soil Dynamics and Earthquake Engineering*, vol. 120, pp. 345–359, 2019.

[21] J. Chen, H. Yu, A. Bobet, and Y. Yuan, "Shaking table tests of transition tunnel connecting TBM and drill-and-blast tunnels," *Tunnelling and Underground Space Technology*, vol. 96, p. 103197, 2020.

[22] Ministry of Housing and Urban-Rural Development of the People's Republic of China, *Code for Seismic Design of Urban Rail Transit Structures, GB50909-2014*, China Project Press, Beijing, China, 2014, in Chinese.

[23] Ministry of Housing and Urban-Rural Development of the People's Republic of China, *Code for Seismic Design of Buildings, GB 50011-2010*, Chinese Architectural Industry Press, Beijing, China, 2010, in Chinese.

[24] X. Zhang, X. Li, G. Chen et al., "An improved method of the calculation of equivalent nodal forces in viscous-elastic artificial boundary," *Chinese Journal of Theoretical and Applied Mechanics*, vol. 48, no. 5, pp. 1126–1135, 2016, in Chinese.

[25] R. M. Pyke, M. J. Pender, and F. E. Richart Jr, "Nonlinear soil models for irregular cyclic loadings," *Journal of Geotechnical Engineering*, vol. 105, no. 6, pp. 715–726, 1979.

[26] G. Chen, D. Jin, J. Zhu, J. Shi, and X. Li, "Nonlinear analysis on seismic site response of fuzhou basin, China," *Bulletin of the Seismological Society of America*, vol. 105, no. 2, pp. 928–949, 2015.

[27] G. Chen, S. Chen, X. Zuo et al., "Shaking-table tests and numerical simulations on a subway structure in soft soil," *Soil Dynamics and Earthquake Engineering*, vol. 76, pp. 13–28, 2015.

[28] D. Zhao, B. Ruan, G. Chen et al., "Validation of the modified irregular loading-reloading rules based on Davidenkov skeleton curve and its equivalent strain algorithm implemented in ABAQUS," *Chinese Journal of Geotechnical Engineering*, vol. 39, no. 5, pp. 888–895, 2017, in Chinese.

[29] W. Chen, D. Jeng, W. Chen, G. Chen, and H. Zhao, "Seismic-induced dynamic responses in a poro-elastic seabed: solutions of different formulations," *Soil Dynamics and Earthquake Engineering*, vol. 131, Article ID 106021, 2020.

[30] I. Anastasopoulos, N. Gerolymos, V. Drosos, R. Kourkoulis, T. Georgarakos, and G. Gazetas, "Nonlinear response of deep immersed tunnel to strong seismic shaking," *Journal of Geotechnical and Geoenvironmental Engineering*, vol. 133, no. 9, pp. 1067–1090, 2007.

[31] Z. Chen and J. Wei, "Correlation between ground motion parameters and lining damage indices for mountain tunnels," *Natural Hazards*, vol. 65, no. 3, pp. 1683–1702, 2013.

[32] Z. Chen, W. Chen, Y. Li, and Y. Yuan, "Shaking table test of a multi-story subway station under pulse-like ground motions," *Soil Dynamics and Earthquake Engineering*, vol. 82, pp. 111–122, 2016.